2650 *Chem. Mater.* **2009,** *21,* 2650–2660
DOI:10.1021/cm803409q

CHEMISTRY OF MATERIALS
Article

New Semiconducting Polymers Containing 3,6-Dimethyl(thieno[3,2-*b*]-thiophene or selenopheno[3,2-*b*]selenophene) for Organic Thin-Film Transistors

Hoyoul Kong,[†] Young Kwan Jung,[†] Nam Sung Cho,[‡] In-Nam Kang,[§] Jong-Hwa Park,[†] Shinuk Cho,*[,‡] and Hong-Ku Shim*[,†]

[†]*Department of Chemistry, Korea Advanced Institute of Science and Technology (KAIST), 373-1 Guseong-Dong, Yuseong-Gu, Daejeon 305-701, Korea,* [‡]*Center for Polymers and Organic Solids, University of California at Santa Barbara, Santa Barbara, California 93106-5090, and* [§]*Department of Chemistry, The Catholic University of Korea, Bucheon, Gyeonggi-do 420-743, Korea*

Received December 17, 2008. Revised Manuscript Received April 22, 2009

A series of new organic semiconducting polymers containing the fused aromatic rings 3,6-dimethylthieno[3,2-*b*]thiophene or 3,6-dimethylselenopheno[3,2-*b*]selenophene as core units were successfully synthesized via oxidative coupling reactions. These core units have the adva3ntage of requiring one-step synthesis. Two polymers containing these core units, poly(2,5-bis(3-dodecylthiophen-2-yl)-3,6-dimethylthieno[3,2-*b*]thiophene) (**PmT**) and poly(2,2′-(3,6-dimethylselenopheno[3,2-*b*]selenophene-2,5-diyl)bis(3-dodecylthiophene)) (**PmSe**), exhibited very poor thin-film transistor (TFT) performances because of the distortion of the core units caused by inter- and intramolecular repulsion between long dodecyl side chains and methyl chains attached to the core units. In contrast, poly(2,5-bis(3′-dodecyl-2,2′-bithiophen-5-yl)-3,6-dimethylthieno[3,2-*b*]thiophene) (**PTmT**) and poly(5′,5″-(3,6-dimethylselenopheno[3,2-*b*]selenophene-2,5-diyl)bis(3-dodecyl-2,2′-bithiophene)) (**PTmSe**) contain additional unsubstituted thiophene rings next to the fused aromatic core units. **PTmT** and **PTmSe** exhibited much more ordered intermolecular structures than **PmT** and **PmSe** because the unsubstituted thiophene rings diminish the distortion of the core units caused by the repulsion of the methyl chains attached to the fused aromatic ring and enable intermolecular interdigitation of the dodecyl side chains of neighboring polymer main backbones. Because of the improved intermolecular ordering, **PTmT** and **PTmSe** exhibited relatively high performance in field effect transistors. The carrier mobilities (μ) of these polymers were 0.03−0.04 $cm^2\ V^{-1}\ s^{-1}$ with an on/off ratio of approximately 10^6, that is, TFT performance parameters that are remarkably better than those of **PmT** ($\mu = 8.1 \times 10^{-7}\ cm^2\ V^{-1}\ s^{-1}$) and **PmSe** ($\mu = 6.4 \times 10^{-6}\ cm^2\ V^{-1}\ s^{-1}$). In addition, **PTmT** and **PTmSe** devices exhibited good thermal stability. Thus, control of the core units is very important in the design of semiconducting polymers with well ordered intermolecular packing for achieving high performance TFTs.

Introduction

Research on organic thin-film transistors (OTFTs) has been a focus of recent interest with the goal of replacing conventional inorganic amorphous silicon TFTs. TFTs based on soluble organic semiconductors offer promise for use in applications such as low cost memory devices, smart cards, and the driving circuits (backplanes) for large-area electronic devices.[1−12] Polymer semiconductors have been the subject of particular attention because of their superior mechanical stability and processability. Furthermore, recent improvements in the charge carrier mobilities and stabilities of devices fabricated with semiconducting polymers have resulted in TFT characteristics as good as those of vacuum-deposited oligomers.[13−15] To obtain high mobilities, the polymer semiconductors must be well ordered when processed from solution. Most studies in this

*To whom correspondence should be addressed. E-mail: hkshim@kaist.ac.kr (H.-K.S.), sucho@physics.ucsb.edu (S.C.). Phone: +82-42-350-2827 (H.-K.S.), +1-805-893-3054 (S.C.). Fax: +82-42-350-2810 (H.-K.S.), +1-805-893-4755 (S.C.).

(1) Kelley, T. W.; Baude, P. F.; Gerlach, C.; Ender, D. E.; Muyres, D.; Haase, M. A.; Vogel, D. E.; Theiss, S. D. *Chem. Mater.* **2004**, *16*, 4413.
(2) Dimitrakopoulos, C. D.; Malenfant, P. R. L. *Adv. Mater.* **2002**, *14*, 99.
(3) Bendikov, M.; Wudl, F.; Perepichka, D. F. *Chem. Rev.* **2001**, *113*, 1069.
(4) Horowitz, G. *Adv. Mater.* **1998**, *10*, 365.
(5) Sirringhaus, H.; Tessler, N.; Friend, R. H. *Science* **1998**, *281*, 1741.
(6) Sirringhaus, H. *Adv. Mater.* **2005**, *17*, 2411.
(7) Bao, Z. *Adv. Mater.* **2000**, *12*, 227.
(8) Forrest, S. R. *Nature* **2004**, *428*, 911.
(9) Mushrush, M.; Facchetti, A.; Lefenfeld, M.; Katz, H. E.; Marks, T. J. *J. Am. Chem. Soc.* **2003**, *125*, 9414.
(10) Babel, A.; Wind, J. D.; Jenekhe, S. A. *Adv. Funct. Mater.* **2004**, *14*, 891.
(11) Li, X.-C.; Sirringhaus, H.; Garnier, F.; Holmes, A. B.; Moratti, S. C.; Feeder, N.; Clegg, W.; Teat, S. J.; Friend, R. F. *J. Am. Chem. Soc.* **1998**, *120*, 2206.
(12) Ahmed, E.; Briseno, A. L.; Xia, Y.; Jenekhe, S. A. *J. Am. Chem. Soc.* **2008**, *130*, 1118.
(13) van Breemen, A. J. J. M.; Herwig, P. T.; Chlon, C. H. T.; Sweelssen, J.; Schoo, H. F. M.; Benito, E. M.; de Leeuw, D. M.; Tanase, C.; Wildeman, J.; Blom, P. W. M. *Adv. Funct. Mater.* **2005**, *15*, 872.
(14) Yang, H.; Shin, T. J.; Yang, L.; Cho, K.; Ryu, C. Y.; Bao, Z. *Adv. Funct. Mater.* **2005**, *15*, 671.
(15) Usta, H.; Lu, G.; Facchetti, A.; Marks, T. J. *J. Am. Chem. Soc.* **2006**, *128*, 9034.

Published on Web 05/14/2009

area have focused on polythiophene derivatives with regioregular long alkyl side chains added to give both good solubility and good intermolecular alignment (through interdigitated ordering of the side chains). Many research groups have reported high charge carrier mobilities (up to 0.1 $cm^2 V^{-1} s^{-1}$) for regioregular head-to-tail poly(3-hexyl thiophene) (P3HT), depending on the device fabrication conditions.[16−18] Ong and co-workers have reported the synthesis of poly(3,3‴-didodecylquaterthiophene) (PQT-12), with $\mu = 0.14\ cm^2 V^{-1} s^{-1}$ and good oxidative doping stability.[19] McCulloch and co-workers have reported poly(2,5-bis(3-alkylthiophene-2-yl)thieno[3,2-*b*]thiophene) (PBTTT), which incorporates thieno[2,3-*b*]thiophene with sulfur atoms in the *anti* position; PBTTT exhibits a liquid crystalline phase that enables the fabrication of films with high crystallinity. TFTs fabricated with PBTTT yield the highest mobility reported to date, $\mu = 0.6-1.0\ cm^2 V^{-1} s^{-1}$.[20,21] Recently, more semiconducting polymers with rigid core units which exhibit good intermolecular ordering have been reported.[22−24]

Here we report a series of new solution-processable regioregular polymer semiconductors, poly(2,5-bis(3-dodecylthiophen-2-yl)-3,6-dimethylthieno[3,2-b]thiophene) (**PmT**), poly(2,2′-(3,6-dimethylselenopheno[3,2-*b*]selenophene-2,5-diyl)-bis(3-dodecylthiophene)) (**PmSe**), poly(2,5-bis(3′-dodecyl-2,2′-bithiophen-5-yl)-3,6-dimethylthieno[3,2-*b*]thiophene) (**PTmT**), and poly(5′,5″-(3,6-dimethylselenopheno[3,2-*b*]selenophene-2,5-diyl)bis(3-dodecyl-2,2′-bithiophene)) (**PTmSe**), which contain 3,6-dimethylthieno[3,2-*b*]-thiophene or 3,6-dimethylselenopheno-[3,2-*b*]selenophene as core units. These two fused aromatic core units can be obtained with practical one-pot synthesis.[25] In addition, **PTmT** and **PTmSe** exhibited much more ordered intermolecular structures than **PmT** and **PmSe** because of the additional thiophene rings next to fused aromatic core units. These polymers were designed according to the following structural considerations. First, we designed **PmT** to investigate the effects of attaching methyl groups to the thieno[3,2-*b*]thiophene core unit. Second, **PmSe** and **PTmSe** were designed to compare the effects of selenium and sulfur atoms in the fused aromatic cores. Lastly and most importantly, we designed **PTmT** and **PTmSe** to improve intermolecular interaction by inserting additional thiophene rings next to the fused aromatic core units along the polymer main backbone.

Experimental Section

Materials. Triethylamine (TEA), *n*-butyllithium, 2-isopropoxy-4,4, 5,5-tetramethyl-1,3,2-dioxaborolane, 2-bromothiophene, chlorobenzene, iron(III) chloride ($FeCl_3$), [1.1′-bis-(diphenylphosphino)-ferrocene]dichloropalladium (II) (Pd(dppf)Cl_2), tetrakis(triphenylphosphine)palladium ($Pd(PPh_3)_4$), and Aliquat336 were obtained from Aldrich Chemical. Magnesium (purum for Grignard reactions) was purchased from Fluka, and *N*-bromosuccinimde (NBS) was purchased from Acros. Chloroform, methylene chloride, tetrahydrofuran (THF), *N,N*-dimethylformamide (DMF), and toluene were obtained from Junsei Chemical. All reagents and solvents were purchased commercially, of analytical-grade quality, and used without further purification.

Measurements. The ^1H and ^{13}C NMR spectra were recorded using a Bruker AVANCE 400 spectrometer, with tetramethylsilane as an internal reference. Elemental analysis was performed using an EA 1110 Fisons analyzer. Melting Point (mp) was measured using an Electrothermal 9100. The number- and weight-average molecular weights of the polymers were determined with gel permeation chromatography (GPC) by using a Viscotek T60A instrument with polystyrene as the standard. Thermogravimetric analysis (TGA) was carried out by using a TA Q500 analyzer with a heating rate of 10 °C/min under a nitrogen atmosphere. Differential scanning calorimetry (DSC) measurements were performed with a TA Q100 instrument and operated under a nitrogen atmosphere at a heating rate of 10 °C/min. The UV−vis spectra were recorded with a Jasco V-530 UV/vis spectrometer, and the photoluminescence (PL) spectra were recorded with a Spex Fluorolog-3 spectrofluorometer (model FL3-11). Cyclic voltammetry (CV) was performed on an AUTOLAB/PG-STAT12 system with a three-electrode cell in a 0.10 M solution of Bu_4NBF_4 in acetonitrile at a scan rate of 50 mV/s. A film of each polymer was coated onto a Pt wire electrode by dipping the electrode into a solution of the polymer. X-ray diffraction (XRD) measurements were carried out on a Panalytical X'pert Pro (PW 3040) with a Cu Kα source ($\lambda = 1.5405$ Å) in air. AFM (Multimode IIIa, Digital Instruments) operating in tapping-mode was used to image the surface morphologies of these semiconductors. The electrical characteristics of the TFTs were determined with Keithley 2400 and 236 source/measure units. In all measurements, the channel length (L) was 50 μm and the channel width (W) was 1500 μm. The field-effect mobilities were extracted in the saturation regime for each polymer from the slope of the source-drain current.

Synthesis of Materials. *3,6-Dimethylthieno[3,2-b]thiophene (**1**) and 3,6-Dimethylselenopheno[3,2-b]selenophene (**2**).* These compounds were prepared in accordance with the literature methods.[25]

*2,5-Dibromo-3,6-dimethylthieno[3,2-b]thiophene (**3**).* To a stirred solution of **1** (2.0 g, 11.89 mmol) in chloroform-acetic acid (1:1 v/v, 80 mL) was added *N*-bromosuccinimide (NBS) (4.45 g, 24.96 mmol). The mixture was stirred at room temperature (RT) for 3 h, and then poured into water (100 mL) and extracted with dichloromethane. The extract was successively washed with water. After drying over anhydrous magnesium sulfate ($MgSO_4$), the solvent was removed by rotary evaporation, and the residue was purified by column chromatography on silica gel with hexane as eluent to afford compound **3**. Yield: 2.35 g (61%).

(16) Zaumseil, J.; Sirringhaus, H. *Chem. Rev.* **2007**, *107*, 1296.
(17) Sirringhaus, H.; Brown, P. J.; Friend, R. H.; Nielsen, M. M.; Bechgaard, K.; Langeveld-Voss, B. M. W.; Spiering, A. J. H.; Janssen, R. A. J.; Meijer, E. W.; Herwig, P.; de Leeuw, D. M. *Nature* **1999**, *401*, 685.
(18) Chang, J. F.; Sun, B. Q.; Breiby, D. W.; Nielsen, M. M.; Solling, T. I.; Giles, M.; McCulloch, I.; Sirringhaus, H. *Chem. Mater.* **2004**, *16*, 4772.
(19) Ong, B. S.; Wu, L. Y.; Liu, P.; Gardner, S. *J. Am. Chem. Soc.* **2004**, *126*, 3378.
(20) McCulloch, I.; Heeney, M.; Bailey, C.; Genevicius, K.; Macronald, I.; Shkunov, M.; Sparrowe, D.; Tierney, S.; Wagner, R.; Zhang, W.; Chabinyc, M. L.; Kline, R. J.; Mcgehee, M. D.; Toney, M. F. *Nat. Mater.* **2006**, *5*, 328.
(21) Hamadani, B. H.; Gundlach, D. J.; McCulloch, I.; Heeney, M. *Appl. Phys. Lett.* **2007**, *91*, 243512.
(22) Li, J.; Qin, F.; Li, C. M.; Bao, Q.; Chan-Park, M. B.; Zhang, W.; Qin, J.; Ong, B. S. *Chem. Mater.* **2008**, *20*, 2057.
(23) Pan, H.; Li, Y.; Wu, Y.; Liu, P.; Ong, B. S.; Zhu, S.; Xu, G. *J. Am. Chem. Soc.* **2007**, *129*, 4112.
(24) Osaka, I.; Sauvé, G.; Zhang, R.; Kowalewski, T.; McCullough, R. D. *Adv. Mater.* **2007**, *19*, 4160.
(25) Choi, K. S.; Saeada, K.; Dong, H.; Hoshino, M.; Nakayama, J. *Heterocycles* **1994**, *38*, 143.

^{1}H NMR ($CDCl_3$, 400 MHz, δ): 2.23 (s, 6H); ^{13}C NMR ($CDCl_3$, 400 MHz, δ): 136.49, 129.73, 109.72, 14.11; mp 158 °C; EIMS (m/z) 325 [M^+]; Anal. Calcd for $C_8H_6Br_2S_2$: C 29.47, H 1.85, S 19.67; found: C 29.49, H 1.86, S 19.70.

*2,5-Dibromo-3,6-dimethylselenopheno[3,2-b]selenophene (**4**).* The compound was synthesized using the same method as for compound **3**, using compound **2** (2.47 g, 9.43 mmol), NBS (3.53 g, 19.81 mmol), and 60 mL of chloroform-acetic acid (1:1 v/v). After drying, the product was purified by column chromatography on silica gel with hexane as eluent. Yield: 2.46 g (62%). ^{1}H NMR ($CDCl_3$, 400 MHz, δ): 2.21 (s, 6H); ^{13}C NMR ($CDCl_3$, 400 MHz, δ): 138.28, 134.66, 109.99, 16.37; mp 167 °C; EIMS (m/z) 420 [M^+]; Anal. Calcd for $C_8H_6Br_2Se_2$: C 22.89, H 1.44; found: C 22.83, H 1.40.

*2-(3-Dodecylthiophen-2-yl)-4,4,5,5-tetramethyl-1,3,2-dioxaborolane (**5**).* To a solution of 2-bromo-3-dodecylthiophene (5.78 g, 17.43 mmol) in THF (70 mL) at −78 °C was added 7.32 mL (18.30 mmol) of *n*-butyllithium (2.5 M in hexane) by syringe. The mixture was stirred at −78 °C for 2 h. 2-Isopropoxy-4,4,5,5,-tetramethyl-1,3,2-dioxaborolane (4.46 mL, 21.79 mmol) was added to the solution, and the resulting mixture was stirred at −78 °C for 1 h, warmed to room temperature, and stirred for a further 12 h. The mixture was poured into water, extracted with ether, and dried over anhydrous $MgSO_4$. The solvent was removed via rotary evaporation, and the residue was purified by column chromatography on silica gel with hexane and triethylamine (TEA) (50:1 [v/v]) as eluent to give compound **5**. Yield: 3.72 g (57%). ^{1}H NMR ($CDCl_3$, 400 MHz, δ): 7.46 (d, 1H), 7.01 (d, 1H), 2.89 (t, 2H), 1.59 (m, 2H), 1.33 (m, 30H), 0.89 (t, 3H); ^{13}C NMR ($CDCl_3$, 400 MHz, δ): 154.63, 131.21, 130.21, 83.44, 31.91, 31.81, 30.11, 29.68, 29.65, 29.62, 29.45, 29.34, 29.29, 24.75, 22.66, 14.07; Anal. Calcd for $C_{22}H_{39}BO_2S$: C 69.83, H 10.39, S 8.47; found: C 69.26, H 10.06, S 8.29.

*2,5-Bis(3-dodecylthiophen-2-yl)-3,6-dimethylthieno[3,2-b]thiophene (**6**).* To a stirred mixture of **3** (1.04 g, 3.19 mmol), 2-(3-dodecylthiophen-2-yl)-4,4,5,5-tetramethyl-1,3,2-dioxaborolane **(5)** (2.78 g, 7.34 mmol), tetrakis(triphenylphosphine)palladium (0.31 g, 0.26 mmol), and Aliquat 336 (0.026 g, 0.064 mmol) in 12.44 mL of anhydrous toluene was added 2 M aqueous sodium carbonate solution (4.15 mL). The solution was refluxed with vigorous stirring for 20 h under a nitrogen atmosphere. The mixture was poured into water (100 mL) and extracted with dichloromethane. The extract was then successively washed with water and brine. After drying over anhydrous $MgSO_4$, the solvent was evaporated, and the residue was purified by column chromatography on silica gel with hexane as eluent to afford compound **6**. Yield: 1.53 g (72%). ^{1}H NMR ($CDCl_3$, 400 MHz, δ): 7.32 (d, 2H), 6.99 (d, 2H), 2.57 (t, 4H), 2.24 (s, 6H), 1.57 (m, 4H), 1.23 (m, 36H), 0.86 (t, 6); ^{13}C NMR ($CDCl_3$, 400 MHz, δ): 142.65, 139.22, 129.81, 129.41, 129.22, 128.70, 125.83, 31.91, 30.67, 29.65, 29.62, 29.55, 29.44, 29.40, 29.34, 28.89, 22.68, 14.11, 13.78 ; mp 58 °C; MS (MALDI-TOF) 669 [M^+]; Anal. Calcd for $C_{40}H_{60}S_4$: C 71.80, H 9.04, S 19.17; found: C 71.81, H 9.07, S 19.13.

*2,2′-(3,6-Dimethylselenopheno[3,2-b]selenophene-2,5-diyl)bis(3-dodecylthiophene) (**7**).* The compound was synthesized using the same method as for compound **6** with compound **4** (1.27 g, 3.04 mmol), compound **5** (2.64 g, 6.98 mmol), tetrakis (triphenylphosphine)palladium (0.28 g, 0.24 mmol), Aliquat 336 (0.025 g, 0.06 mmol), 11.86 mL of anhydrous toluene and 2 M aqueous sodium carbonate solution (3.96 mL). After column chromatography on silica gel with hexane as eluent, compound **7** was obtained. Yield: 1.62 g (70%). ^{1}H NMR ($CDCl_3$, 400 MHz, δ): 7.30 (d, 2H), 6.96 (d, 2H), 2.56 (t, 4H), 2.19 (s, 6H), 1.55 (m, 4H), 1.24 (m, 36H), 0.87 (t, 6); ^{13}C NMR ($CDCl_3$, 400 MHz, δ): 141.98, 141.46, 134.22, 132.39, 131.22, 128.73, 125.66, 31.91, 30.58, 29.65, 29.62, 29.55, 29.46, 29.43, 29.34, 28.96, 22.68, 15.94, 14.10 ; mp 73 °C; MS (MALDI-TOF) 763 [M^+]; Anal. Calcd for $C_{40}H_{60}S_2Se_2$: C 62.97, H 7.93, S 8.41; found: C 62.99, H 7.97, S 8.40.

*3,6-Dimethyl-2,5-di(thiophen-2-yl)thieno[3,2-b]thiophene (**8**).* A solution of 2-bromothiophene (1.92 g, 11.76 mmol) in 15 mL anhydrous tetrahydrofuran (THF) was added dropwise to magnesium (0.39 g, 15.68 mmol) in anhydrous THF (7 mL), and the mixture was refluxed for 2 h at 60 °C under nitrogen gas. The resulting mixture was added slowly to a solution of compound **3** (1.28 g, 3.92 mmol) and Pd(dppf)Cl_2 (0.07 g, 0.079 mmol) in anhydrous THF (25 mL) at 0 °C. The mixture was refluxed for 12 h at 60 °C, after which HCl solution (10%) was added. The mixture was washed with ethyl acetate, NaOH (10%), $NaHCO_3$ (1M), and water. After drying over anhydrous $MgSO_4$, the solvent was evaporated. Purification on a silica column with 1:1 hexane/dichloromethane as eluent, followed by recrystallization from dichloromethane/methanol, gave compound **9**. Yield: 1.08 g (83%). ^{1}H NMR ($CDCl_3$, 400 MHz, δ): 7.33 (d, 2H), 7.17 (d, 2H), 7.08 (t, 2H), 2.46 (s, 6H); ^{13}C NMR ($CDCl_3$, 400 MHz, δ): 138.83, 136.92, 131.63, 127.51, 126.31, 125.65, 125.46, 14.36; mp 156 °C; MS (MALDI-TOF) 332 [M^+]; Anal. Calcd for $C_{16}H_{12}S_4$: C 57.79, H 3.64, S 38.57; found: C 57.01, H 3.59, S 37.98.

*2,2′-(3,6-Dimethylselenopheno[3,2-b]selenophene-2,5-diyl)dithiophene (**9**).* The compound was synthesized using the same method as for compound **8** with 2-bromothiophene (2.57 g, 15.72 mmol), magnesium (0.51 g, 20.96 mmol), compound **4** (2.2 g, 5.24 mmol), and Pd(dppf)Cl_2 (0.09 g, 0.105 mmol). The mixture was refluxed for 12 h at 60 °C, after which HCl solution (10%) was added. The mixture was washed with ethyl acetate, NaOH (10%), $NaHCO_3$ (1M), and water. After drying over anhydrous $MgSO_4$, the solvent was evaporated. Purification on a silica column with 1:1 hexane/dichloromethane as eluent, followed by recrystallization from dichloromethane/methanol gave compound **9**. Yield: 1.75 g (79%). ^{1}H NMR ($CDCl_3$, 400 MHz, δ): 7.32 (d, 2H), 7.12 (d, 2H), 7.06 (t, 2H), 2.43 (s, 6H); ^{13}C NMR ($CDCl_3$, 400 MHz, δ): 140.94, 138.65, 133.83, 131.01, 127.58, 126.06, 125.73, 16.57; mp 179 °C; MS (MALDI-TOF) 426 [M^+]; Anal. Calcd for $C_{16}H_{12}S_2Se_2$: C 45.08, H 2.84, S 15.04; found: C 45.11, H 2.88, S 15.02.

*2,5-Bis(5-bromothiophen-2-yl)-3,6-dimethylthieno[3,2-b]thiophene (**10**).* To a stirred solution of compound **8** (1.03 g, 3.10 mmol) in *N,N*-dimethylformamide (DMF)-chloroform (1:2 v/v, 35 mL), NBS (1.16 g, 6.51 mmol) was added. The mixture was stirred at RT for 3 h, and then poured into water (100 mL) and extracted with dichloromethane. The extract was successively washed with water. After drying over anhydrous $MgSO_4$, the solvent was removed by rotary evaporation, and the residue was purified by recrystallization from dichloromethane/methanol to obtain compound **10**. Yield: 1.26 g (83%). ^{1}H NMR ($CDCl_3$, 400 MHz, δ): 7.03 (d, 2H), 6.90 (d, 2H), 2.41 (s, 6H); ^{13}C NMR ($CDCl_3$, 400 MHz, δ): 139.00, 138.24, 131.03, 130.37, 126.86, 126.00, 112.30, 14.29; mp 171 °C; MS (MALDI-TOF) 490 [M^+]; Anal. Calcd for $C_{16}H_{10}Br_2S_4$: C 39.19, H 2.06, S 26.16; found: C 38.79, H 2.01, S 26.05.

*5,5′-(3,6-Dimethylselenopheno[3,2-b]selenophene-2,5-diyl)bis(2-bromothiophene) (**11**).* The compound was synthesized using the same method as for compound **11** with compound **9** (0.9 g, 2.11 mmol), DMF-chloroform (1:2 v/v, 30 mL), and NBS (0.77 g, 4.33 mmol). The mixture was stirred at RT for 3 h, and then poured into water (100 mL) and extracted

Scheme 1. Synthetic Routes for PmT, PmSe, PTmT, and PTmSe

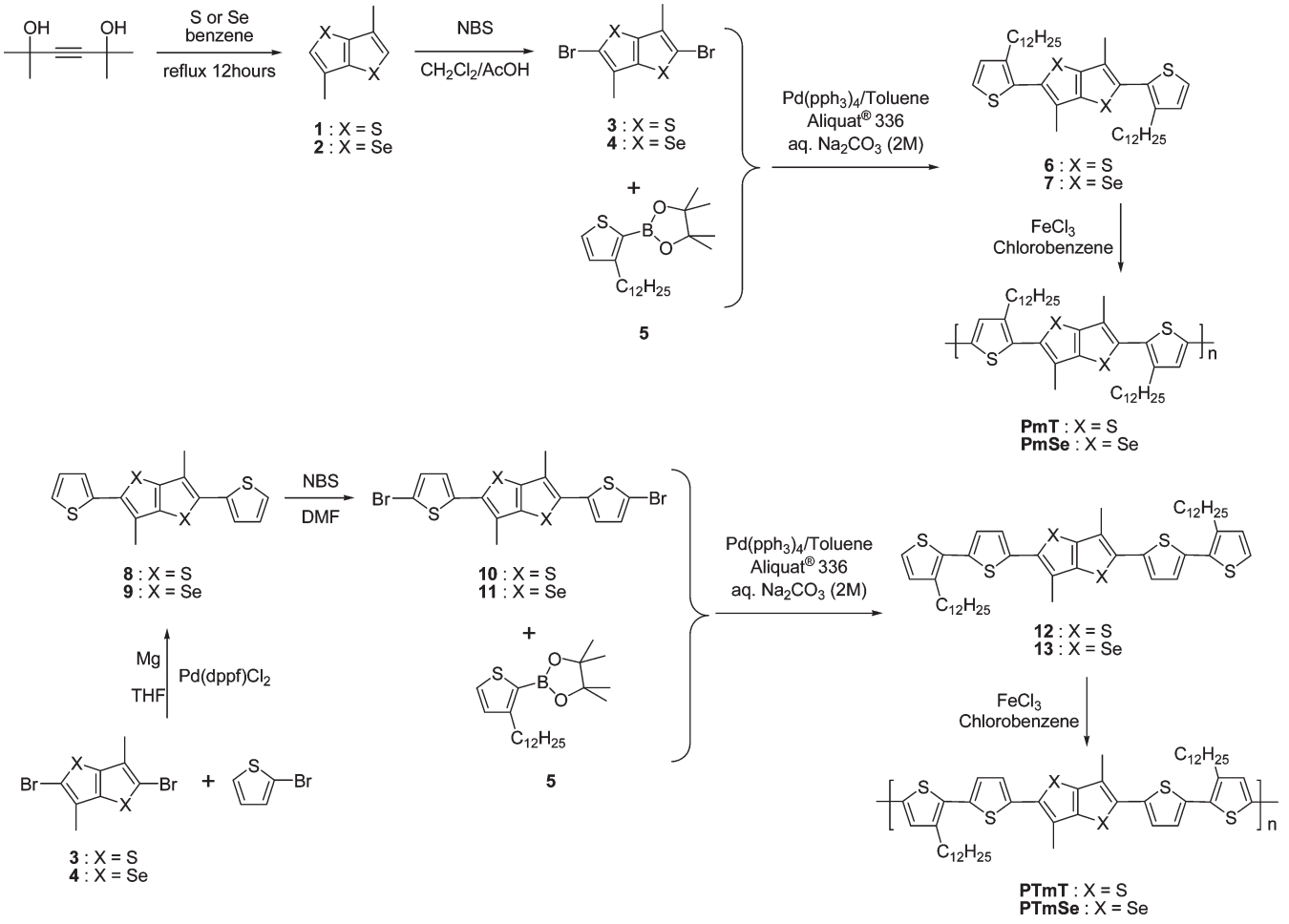

with dichloromethane. The extract was successively washed with water. After drying over anhydrous $MgSO_4$, the solvent was removed by rotary evaporation, and the residue was purified by recrystallization from dichloromethane/methanol to obtain compound **11**. Yield: 1.03 g (84%). ^{1}H NMR ($CDCl_3$, 400 MHz, δ): 7.01 (d, 2H), 6.85 (d, 2H), 2.38 (s, 6H); ^{13}C NMR ($CDCl_3$, 400 MHz, δ): 141.11, 139.94, 133.09, 131.53, 130.42, 126.32, 112.53, 16.51; mp 198 °C; MS (MALDI-TOF) 584 [M^+]; Anal. Calcd for $C_{16}H_{10}Br_2S_2Se_2$: C 32.90, H 1.73, S 10.98; found: C 32.94, H 1.77, S 10.99.

*2,5-Bis(3′-dodecyl-2,2′-bithiophen-5-yl)-3,6-dimethylthieno-[3,2-b]thiophene (**12**)*. The compound was synthesized using the same method as for compound **6** with compound **10** (1.25 g, 2.55 mmol), compound **5** (2.22 g, 5.86 mmol), tetrakis(triphenylphosphine)palladium (0.24 g, 0.21 mmol), Aliquat 336 (0.021 g, 0.05 mmol), 9.96 mL of anhydrous toluene, and 2 M aqueous sodium carbonate solution (3.32 mL). The solution was refluxed with vigorous stirring for 20 h under a nitrogen atmosphere. The mixture was poured into water (100 mL) and extracted with dichloromethane. The extract was then successively washed with water and brine. After drying over anhydrous MgSO4, the solvent was evaporated. The residue was purified by column chromatography on silica gel with 1:1 hexane/dichloromethane as eluent and then further recrystallized from dichloromethane/methanol to afford compound **12**. Yield: 1.43 g (67%). ^{1}H NMR ($CDCl_3$, 400 MHz, δ): 7.16 (d, 2H), 7.12 (d, 2H), 7.07 (d, 2H), 6.92 (d, 2H), 2.79 (t, 4H), 2.50 (s, 6H), 1.64 (m, 4H), 1.29 (m, 36H), 0.87 (t, 6H); ^{13}C NMR ($CDCl_3$, 400 MHz, δ): 140.04, 139.20, 136.86, 136.66, 131.86, 130.37, 130.06, 126.48, 126.32, 125.92, 123.93, 31.94, 30.69, 29.69, 29.66, 29.61, 29.54, 29.47, 29.34, 29.29, 22.66, 14.46, 14.00; mp 97 °C; MS (MALDI-TOF) 832 [M^+]; Anal. Calcd for $C_{48}H_{64}S_6$: C 69.18, H 7.74, S 23.08; found: C 68.76, H 7.35, S 22.54.

*5′,5″-(3,6-Dimethylselenopheno[3,2-b]selenophene-2,5-diyl)-bis(3-dodecyl-2,2′-bithiophene) (**13**)*. The compound was synthesized using the same method as for compound **12** with compound **11** (1.00 g, 1.71 mmol), compound **5** (1.50 g, 3.94 mmol), tetrakis (triphenylphosphine)palladium (0.16 g, 0.14 mmol), Aliquat 336 (0.014 g, 0.04 mmol), 8.00 mL of anhydrous toluene, and 2 M aqueous sodium carbonate solution (2.23 mL). The solution was refluxed with vigorous stirring for 20 h under a nitrogen atmosphere. The mixture was poured into water (100 mL) and extracted with dichloromethane. The extract was then successively washed with water and brine. After drying over anhydrous MgSO4, the solvent was evaporated. The residue was purified by column chromatography on silica gel with 1:1 hexane/dichloromethane as eluent and then further recrystallized from dichloromethane/methanol to afford compound **13**. Yield: 1.03 g (65%). ^{1}H NMR ($CDCl_3$, 400 MHz, δ): 7.17 (d, 2H), 7.06 (d, 4H), 6.93 (d, 2H), 2.77 (t, 4H), 2.47 (s, 6H), 1.64 (m, 4H), 1.29 (m, 36H), 0.86 (t, 6H); ^{13}C NMR ($CDCl_3$, 400 MHz, δ): 141.04, 139.87, 138.35, 136.67, 133.82, 130.94, 130.23, 130.12, 126.23, 126.21, 123.90, 31.93, 30.71, 29.69, 29.67, 29.62, 29.54, 29.46, 29.36, 29.30, 22.69, 16.79, 14.12; mp 109 °C; MS (MALDI-TOF) 927 [M^+]; Anal. Calcd for $C_{48}H_{64}S_4Se_2$: C 62.18, H 6.96, S 13.83; found: C 62.14, H 6.99, S 13.84.

*Poly(2,5-bis(3-dodecylthiophen-2-yl)-3,6-dimethylthieno-[3,2-b]thiophene) (**PmT**)*. **PmT** was synthesized according to the literature method.[26] A solution of compound **6** (0.25 g, 3.79 mmol) in 7.3 mL of chlorobenzene was added dropwise to a stirred mixture of $FeCl_3$ (0.31 g, 1.89 mmol) in 6 mL of chlorobenzene under an argon atmosphere. The resulting mixture was refluxed for 48 h at 65 °C under an argon atmosphere. After cooling to room temperature, the mixture was poured into 150 mL of methanol. The precipitated polymer was collected by filtration and reprecipitation from methanol and acetone. The reprecipitated polymer was filtered and added to a mixture of 200 mL methanol and 50 mL 30% aqueous ammonia solution, and then was stirred for 3 days. The polymer was purified further by washing for 2 days in a Soxhlet apparatus with methanol, acetone, and heptane to remove oligomers and catalyst residues, and by column chromatography with a chloroform/toluene solution of the polymer. The reprecipitation procedure in toluene/methanol was then repeated several times. The final product, a dark yellow polymer (0.08 g), was obtained after drying in vacuo at 60 °C. ^{1}H NMR (TCE, 400 MHz, δ): aromatic; 7.14−7.12 (2H), aliphatic; 2.60−2.58 (4H), 2.35−2.33 (6H), 1.60 (4H), 1.25 (36H), 0.89−0.86 (6H); Anal. Calcd for $C_{40}H_{60}S_4$: C 71.80, H 9.04, S 19.17; found: C 71.89, H 9.08, S 19.20.

*Poly(2,2′-(3,6-dimethylselenopheno[3,2-b]selenophene-2,5-diyl)bis(3-dodecylthiophene)) (**PmSe**)*. **PmSe** was synthesized using the same method as for **PmT** with compound **7** (0.41 g, 0.53 mmol), $FeCl_3$ (0.43 g, 2.65 mmol), and chlorobenzene (18 mL). The final product, a dark yellow polymer (0.19 g), was obtained after drying in vacuo at 60 °C. ^{1}H NMR (TCE, 400 MHz, δ): aromatic; 7.13−7.11 (2H), aliphatic; 2.59−2.54 (4H), 2.31 (6H), 1.63 (4H), 1.26 (36H), 0.90−0.87 (6H); Anal. Calcd for $C_{40}H_{60}S_2Se_2$: C 62.97, H 7.93, S 8.41; found: C 62.99, H 7.98, S 8.43.

*Poly(2,5-bis(3′-dodecyl-2,2′-bithiophen-5-yl)-3,6-dimethylthieno[3,2-b]thiophene) (**PTmT**)*. **PTmT** was synthesized using the same method as for **PmT** with compound **12** (0.30 g, 0.36 mmol), $FeCl_3$ (0.29 g, 1.80 mmol), and chlorobenzene (13 mL). The final product, a dark red polymer (0.13 g), was obtained after drying in vacuo at 60 °C. ^{1}H NMR (TCE, 400 MHz, δ): aromatic; 7.22−7.20 (4H), 7.10 (2H), aliphatic; 2.87−2.85 (4H), 2.59 (6H), 1.79−1.77 (4H), 1.51−1.36 (36H), 0.97−0.94 (6H); Anal. Calcd for $C_{48}H_{64}S_6$: C 69.18, H 7.74, S 23.08; found: C 69.02, H 7.81, S 23.01.

*Poly(5′,5″-(3,6-dimethylselenopheno[3,2-b]selenophene-2,5-diyl)bis(3-dodecyl-2,2′-bithiophene)) (**PTmSe**)*. **PTmSe** was synthesized using the same method as for **PmT** with compound **13** (0.31 g, 0.33 mmol), $FeCl_3$ (0.27 g, 1.67 mmol), and chlorobenzene (12 mL). The final product, a dark red polymer (0.14 g), was obtained after drying in vacuo at 60 °C. ^{1}H NMR (TCE, 400 MHz, δ): aromatic; 7.18−7.07 (4H), 6.83 (2H), aliphatic; 2.87−2.83 (4H), 2.56−2.53 (6H), 1.79−1.74 (4H), 1.44−1.39 (36H), 0.96−0.93 (6H); Anal. Calcd for $C_{48}H_{64}S_4Se_2$: C 62.18, H 6.96, S 13.83; found: C 62.20, H 6.99, S 13.84.

Results and Discussion

Synthesis and Thermal Properties. The syntheses of **PmT**, **PmSe**, **PTmT**, and **PTmSe** are shown in Scheme 1. The monomers 3,6-dimethylthieno[3,2-*b*]thiophene **(1)** and 3,6-dimethylselenopheno[3,2-*b*]selenophene **(2)** were synthesized according to an established method.[25] Because of the nature of the synthesis, methyl groups are attached to the fused rings. However, this route is a very efficient method for the one-step synthesis of fused aromatic rings. In addition, semiconducting polymers containing the fused selenophene ring can be easily prepared via this synthetic method. The final monomers for the polymerizations, 2,5-bis(3-dodecylthiophen-2-yl)-3,6-dimethylthieno[3,2-*b*]-thiophene **(6)**, 2,2′-(3,6-dimethylselenopheno[3,2-*b*]selenophene-2,5-diyl)bis(3-dodecylthiophene) **(7)**, 2,5-bis(3′-dodecyl-2,2′-bithiophen-5-yl)-3,6-dimethylthieno[3,2-*b*]thiophene **(12)**, and 5′,5″-(3,6-dimethylselenopheno[3,2-*b*]-selenophene-2,5-diyl)bis(3-dodecyl-2,2′-bithiophene) **(13)**, were synthesized via Suzuki couplings in the presence of catalytic amounts of $Pd(PPh_3)_4$ and Na_2CO_3 in relatively high yields, from 65 to 72%. The syntheses of the polymers were carried out using $FeCl_3$-mediated oxidative coupling polymerizations in chlorobenzene. These polymers were purified by reprecipitation and Soxhlet extraction with methanol, acetone, and heptane. Their chemical structures were verified with ^{1}H NMR and elemental analysis. The number-average molecular weights (M_n) of **PmT**, **PmSe**, **PTmT**, and **PTmSe** were determined with gel permeation chromatography (GPC) by using a polystyrene standard and found to be 12,100 (M_w/M_n = 1.84), 14,700 (M_w/M_n = 1.93), 13,300 (M_w/M_n = 1.89), and 15,200 (M_w/M_n = 1.83), respectively.

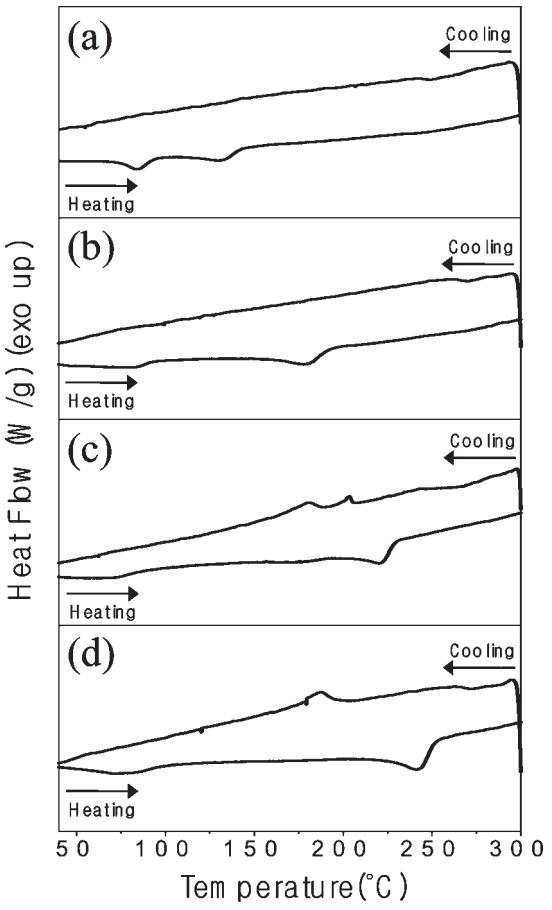

Figure 1. DSC thermograms of (a) **PmT**, (b) **PmSe**, (c) **PTmT**, and (d) **PTmSe** at a temperature ramp 10 °C/min under N_2.

PmT, **PmSe**, **PTmT**, and **PTmSe** were found to exhibit very good thermal stabilities, losing less than 5% of their weight on heating to about 400 °C, as determined with

(26) Pan, H.; Wu, Y.; Li, Y.; Liu, P.; Ong, B. S.; Zhu, S.; Xu, G. *Adv. Funct. Mater.* **2007**, *17*, 3574.

Table 1. Thermal, Optical, and Electrochemical Properties of the Polymers

			absorption λ_{max} (nm) [c]					
polymer	T_1 (°C)[a]	T_2 (°C)[b]	hot solution	solution	film	annealed film	E_g [eV][d]	*IP* [eV][e]
PmT	85, 131	N.A.	380	382	394	396	2.74	5.5
PmSe	85, 178	N.A.	396	398	416	415	2.62	5.6
PTmT	72, 221	179, 203	469, 551, 595	499, 556, 601	552, 598	553, 596	1.94	5.0
PTmSe	73, 243	187	472, 621	495, 568, 621	572, 620	568, 613	1.84	5.1

[a] Endotherms on heating at 10 °C/min. [b] Exotherms on heating at 10 °C/min. [c] Hot solution: dilute chlorobenzene solution at 60 °C; solution: dilute chlorobenzene solution at room temperature; film: thin film spin coated from chlorobenzene solution; annealed film: thin film annealed at 120 °C for 10 min. [d] The optical band gap was determined from the UV−vis absorption onset in the solid state. [e] The IP value of each polymer films was determined from the onset voltage of the first oxidation potential with ferrocene at −4.8 eV.

thermo-gravimetric analysis (TGA) under a nitrogen atmosphere. The differential scanning calorimetry (DSC) (Figure 1 and Table 1) thermograms for the polymers showed two discrete endotherms on heating at 73−85 °C (first transition temperature) and 131−243 °C (second transition temperature), similar to the DSC patterns of other thiophene-based copolymer systems.[19−21,26] In addition, **PTmT** and **PTmSe** showed exothermic peaks on cooling, which mean recrystallization, whereas **PmT** and **PmSe** did not show any exothermic transitions on cooling.

Optical and Electrochemical Properties. The UV−vis absorption and PL spectra of the polymers in dilute chlorobenzene solution and spin-coated thin-films were recorded (Figure 2). The UV−vis absorption maxima of **PmT** and **PmSe** were at 382 nm (hot solution: 380 nm) and 398 nm (hot solution: 396 nm) in solution, and at 394 nm (annealed film: 396 nm) and 416 nm (annealed film: 415 nm) in the film state, respectively (Table 1). For both **PmT** and **PmSe** polymers, when their hot solutions were cooled to room temperature or their thin-films were annealed, there were very small red-shifts in these peaks implying that **PmT** and **PmSe** polymers have very short effective conjugation lengths because of the distortion of the core units containing methyl groups. In the case of PBTTT, the core unit does not contain a methyl group, so the polymer retains its planarity; as a result, its UV−vis absorption maximum is significantly red-shifted to 547 nm.[20] Unlike **PmT** and **PmSe**, **PTmT** and **PTmSe** contain two unsubstituted thiophene rings next to the core unit, and so exhibit significantly different UV−vis spectra. First, the UV−vis absorption peaks of **PTmT** and **PTmSe** in both solution and film were significantly red-shifted and showed well-defined vibronic structures. The latter indicates well ordered intermolecular packing and a longer effective conjugation length than obtained with of **PmT** and **PmSe**. Second, the UV−vis spectrum of **PTmT** and **PTmSe** in hot solution contains strong peak at 469 and 472 nm with weak shoulder absorption at 595 and 621 nm, respectively. When these hot solutions were cooled to room temperature, two new strong shoulder absorptions at 556−568 and 601−621 nm appeared. These two shoulder peaks are consistent with the film UV−vis absorption peaks and indicate a transition from disordered molecular ordering to well-ordered molecular packing at room temperature. Finally, the absorption maxima obtained from thin-films were about 70−80 nm red-shifted with respect to those of the solutions, again implying well organized intermolecular ordering in the solid states.[26] In addition, the UV−vis absorption peaks of **PmSe** and **PTmSe** in both solution and film were about 20 nm red-shifted with respect to those of **PmT** and **PTmT**, which results from the presence of the selenium atoms in its core repeat units. Selenium atoms are more electron rich than sulfur atoms, so aromatic rings containing selenium are more easily delocalized than those containing sulfur atoms.[27−29]

To confirm the improved intermolecular ordering of **PTmT** and **PTmSe**, we determined the PL spectra of solutions with the same concentration as used for the UV−vis spectra. The PL maximum intensities of the cooled solutions were about 60% less than that of hot solutions. This clear indication of excitation quenching of the PL spectrum in dilute solution indicates the presence of strong intermolecular interactions between the polymer chains.

The optical band gaps of the polymers were determined from the UV−vis absorption onsets in the solid state ($E_g = 1240/\lambda_{onset}$ eV). The optical band gaps of **PmT** and **PmSe** were 2.74 and 2.62 eV, respectively. In contrast, **PTmT** and **PTmSe** exhibited very low optical band gaps of 1.94 and 1.84 eV, respectively, that is, the band gaps decrease in the order **PmT** > **PmSe** ≫ **PTmT** > **PTmSe**. The band gap of **PmSe** and **PTmSe** was smaller than that of **PmT** and **PTmT**, respectively, because of the electron-rich selenium atoms in core repeat units. In addition, **PTmT** and **PTmSe** containing unsubstituted thiophenes exhibited much smaller band gaps than those of **PmT** and **PmSe**. The unsubstituted thiophene rings next to the core units of **PTmT** and **PTmSe** increase the effective conjugation length, diminish the distortion of the core units, and provide enough space for the interdigitation of the long alkyl side chains.

We carried out CV measurements on thin-films of the polymers to determine their ionization potentials (IPs, Figure 3). These measurements were performed in an electrolyte solution of 0.1 M tetrabutylammonium tetrafluoroborate ($TBABF_4$) in anhydrous acetonitrile at room temperature under nitrogen gas with a scan rate of 50 mV/s. To convert the measured redox behaviors into IPs, we used an empirical relationship based on the detailed comparison of valence effective Hamiltonian calculations and experi-

(27) Salzner, U.; Lagowski, J. B.; Pickup, P. G.; Poirier, R. A. *Synth. Met.* **1998**, *96*, 177.
(28) Heeney, M.; Zhang, W.; Crouch, D. J.; Chabinyc, M. L.; Gordeyev, S.; Hamilton, R.; Higgins, S. J.; McCulloch, I.; Skabara, P. J.; Sparrowe, D.; Tierney, S. *Chem. Commun.* **2007**, 5061.
(29) Patra, A.; Wijsboom, Y. H.; Zade, S. S.; Li, M.; Sheynin, Y.; Leitus, G.; Bendikov, M. *J. Am. Chem. Soc.* **2008**, *130*, 6734.

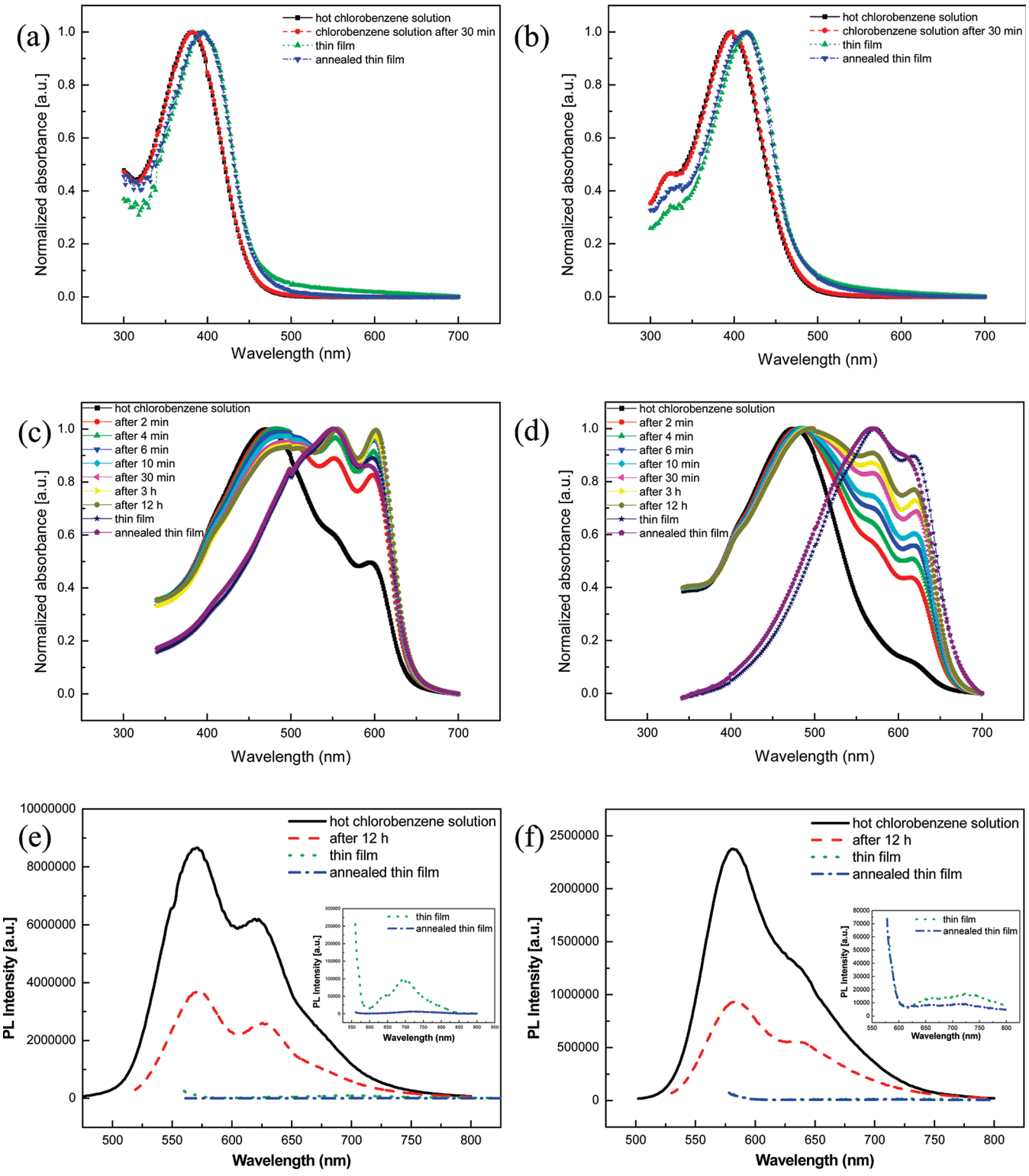

Figure 2. UV−vis absorption spectra of (a) **PmT**, (b) **PmSe**, (c) **PTmT**, and (d) **PTmSe**, and the PL spectra of (e) **PTmT** and (f) **PTmSe** (inset: enlarged film PL spectra).

mental electrochemical measurements and assume that the energy level of ferrocene/ferrocenium is 4.8 eV below the vacuum level.[30,31] The IPs of **PTmT** and **PTmSe** were found to be 5.0 and 5.1 eV, respectively, which matches the work function of gold. These IP values ensure effective hole injection between a gold electrode and the semiconducting layer. The IP of **PTmSe** is higher than that of **PTmT**, which indicates that **PTmSe** has better resistance against oxidative doping than **PTmT**.[32] The IPs of **PmT**

(30) Brédas, J. L.; Silbey, R.; Boudreaux, D. S.; Chance, R. R. *J. Am. Chem. Soc.* **1983**, *105*, 6555.
(31) Pommerehne, J.; Vestweber, H.; Guss, W.; Mahrt, R. F.; Bässler, H.; Porsch, M.; Daub, J. *Adv. Mater.* **1995**, *7*, 551.
(32) Li, Y.; Wu, Y.; Liu, P.; Birau, M.; Pan, H.; Ong, B. S. *Adv. Mater.* **2006**, *18*, 3029.

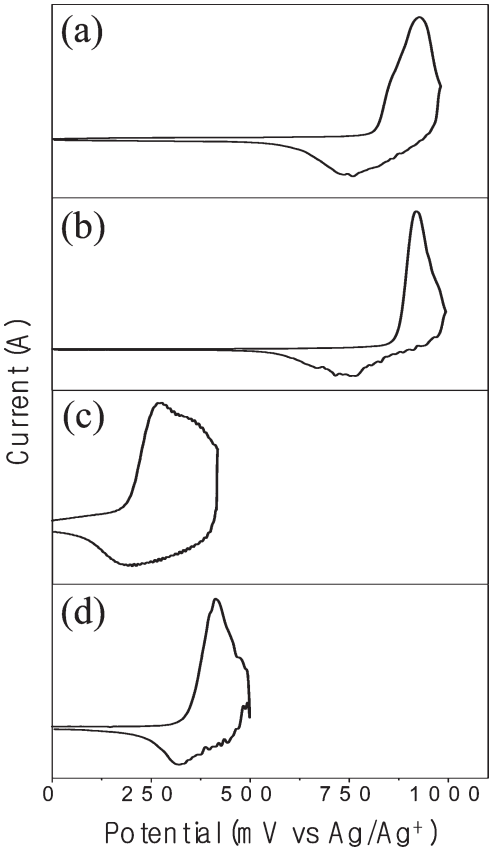

Figure 3. Cyclic voltammograms of (a) **PmT**, (b) **PmSe**, (c) **PTmT**, and (d) **PTmSe**.

and **PmSe** were 5.5 and 5.6 eV, respectively. These higher IP values result in much better stability in oxygen. However, poor hole injection because of higher IP values can result in poor TFT properties.

XRD and Structural Properties. XRD analyses of thin-films were carried out to investigate the structural ordering. Thin-films (thickness of 70−80 nm) were spin-cast onto octyltrichlorosilane (OTS-8) modified Si/SiO_2 substrates and annealed at 120 °C for 10 min. (100) peaks were observed for **PmSe**, **PTmT**, and **PTmSe** at 2θ = 4.53°, 3.18°, and 3.30°, respectively, which correspond to *d*-spacings (the interlayer distance) of 19.50, 27.70, and 26.75 Å, respectively (Figure 4). Note that **PmT** has similar molecular structures to **PmSe**. Nevertheless, no crystalline peak was observed in the thin-film of **PmT**, which means that the thin-film of **PmT** is amorphous. It may be considered that the interlayer ordering of **PmT** is less facilitated than **PmSe** because of the poor electron density of sulfur atom. This result is consistent with the result that (100) peak intensity of **PTmT** is smaller than that of **PTmSe**. Interestingly, the *d*-spacings of **PTmT** and **PTmSe** are significantly longer than that of **PmSe**. It might be because the fused aromatic core units of **PmT** and **PmSe** are much more twisted than those of **PTmT** and **PTmSe**. In addition, in the case of **PTmT** and **PTmSe**, the space between dodecyl-thiophene and methyl chain lengthened by the unsubstituted thiophene ring is about 17.7 Å (d_2), which is longer than d_1 (14.4 Å), and it is sufficient for interdigitation without the repulsion

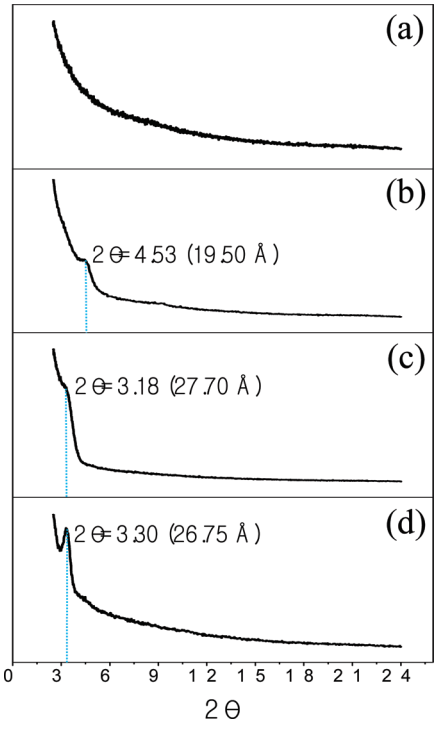

Figure 4. XRD patterns of (a) **PmT**, (b) **PmSe**, (c) **PTmT**, and (d) **PTmSe**.

between the methyl chains and the long dodecyl chains (Figure 5).

To confirm the distortion of the fused aromatic core units for the polymers, we performed quantum chemical calculations using the Gaussian 03 Program[33] by using the hybrid functional B3LYP with the 3-21G* basis set.[34,35] Although many conformers of the polymers exist, to search the more stable conformers, we calculated the relaxed potential energy surface (PES) scans as a function of dihedral angles α or β. As models of the polymers, we used the molecular structures of the compounds consisting of the several polymer units containing butyl-thiophene instead of dodecyl-thiophene. As shown in Figure 6, dihedral angles of stable conformers, α, between fused core unit and polymer backbone for **PmT** and **PmSe** are 70.0°. This angle is much larger than the dihedral angle, β (140 or −40°), for stable conformers of **PTmT** and **PTmSe**. The methyl chains of the fused core ring cause intramolecular repulsion

(33) Frisch, M. J.; Trucks, G. W.; Schlegel, H. B.; Scuseria, G. E.; Robb, M. A.; Cheeseman, J. R.; Montgomery, Jr., J. A.; Vreven, T.; Kudin, K. N.; Burant, J. C.; Millam, J. M.; Iyengar, S. S.; Tomasi, J.; Barone, V.; Mennucci, B.; Cossi, M.; Scalmani, G.; Rega, N.; Petersson, G. A.; Nakatsuji, H.; Hada, M.; Ehara, M.; Toyota, K.; Fukuda, R.; Hasegawa, J.; Ishida, M.; Nakajima, T.; Honda, Y.; Kitao, O.; Nakai, H.; Klene, M.; Li, X.; Knox, J. E.; Hratchian, H. P.; Cross, J. B.; Bakken, V.; Adamo, C.; Jaramillo, J.; Gomperts, R.; Stratmann, R. E.; Yazyev, O.; Austin, A. J.; Cammi, R.; Pomelli, C.; Ochterski, J. W.; Ayala, P. Y.; Morokuma, K.; Voth, G. A.; Salvador, P.; Dannenberg, J. J.; Zakrzewski, V. G.; Dapprich, S.; Daniels, A. D.; Strain, M. C.; Farkas, O.; Malick, D. K.; Rabuck, A. D.; Raghavachari, K.; Foresman, J. B.; Ortiz, J. V.; Cui, Q.; Baboul, A. G.; Clifford, S.; Cioslowski, J.; Stefanov, B. B.; Liu, G.; Liashenko, A.; Piskorz, P.; Komaromi, I.; Martin, R. L.; Fox, D. J.; Keith, T.; Al-Laham, M. A.; Peng, C. Y.; Nanayakkara, A.; Challacombe, M.; Gill, P. M. W.; Johnson, B.; Chen, W.; Wong, M. W.; Gonzalez, C.; and Pople, J. A.; Gaussian 03, Revision C.02; Gaussian, Inc.: Wallingford, CT, 2004.
(34) Becke, A. D. *J. Chem. Phys.* **1993**, *98*, 5648.
(35) Perdew, J. P. *Phys. Rev. B* **1986**, *33*, 8822.

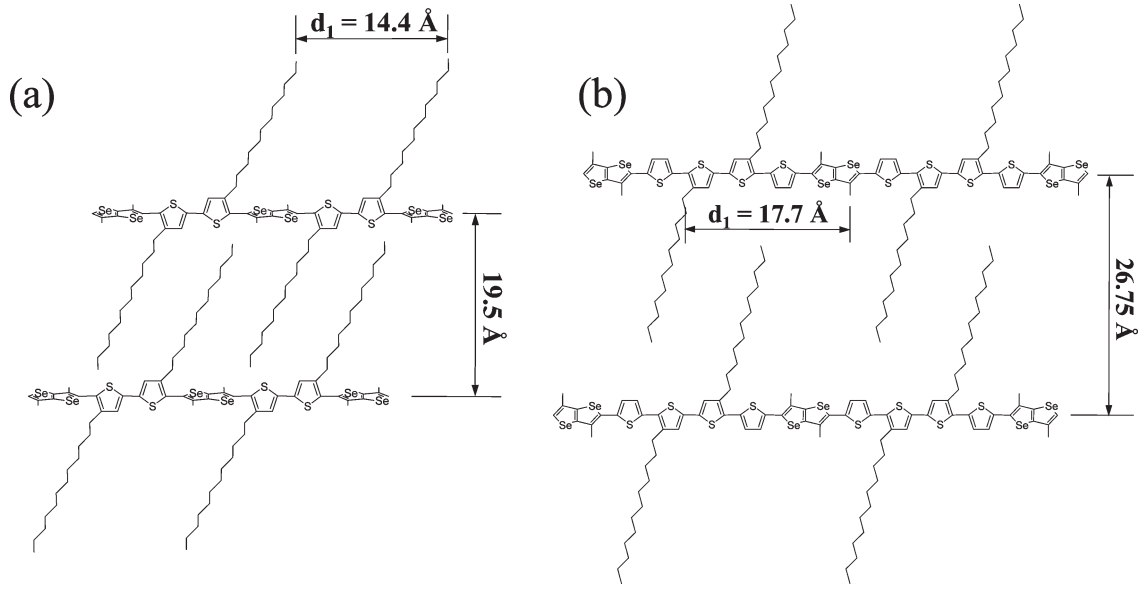

Figure 5. Schematic representations of (a) **PmSe** and (b) **PTmSe**.

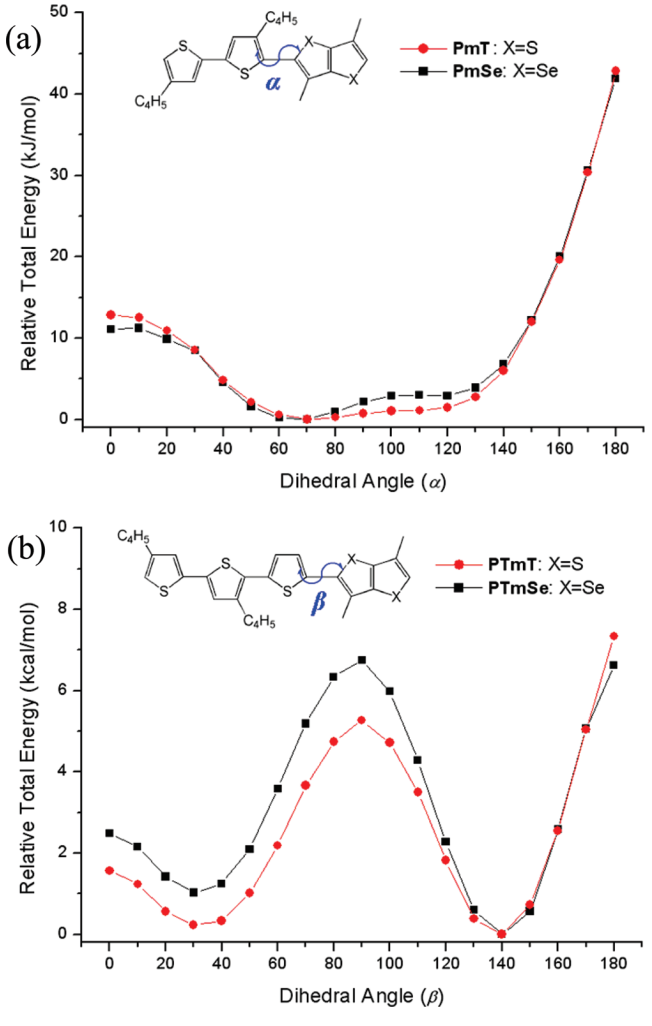

Figure 6. Relaxed PES scan of (a) **PmT** and **PmSe**, and (b) **PTmT** and **PTmSe**. Relative total energies are plotted against the dihedral angle α or *β*, respectively.

with butyl-thiophene and unsubstituted thiophene, for **PmSe** (or **PmT**) and **PTmSe** (or **PTmT**), respectively. The difference of bulkiness between butyl-thiophene and unsubstituted thiophene gives rise to significantly different dihedral angles. In this regard, on the basis of these dihedral angles of the fused core rings, the optimized molecular structures of the several repeating units for the polymers were obtained from the full geometry optimization. As shown in Figure 7, **PTmT** and **PTmSe** containing an unsubstituted thiophene ring exhibited much more planar structures than **PmT** and **PmSe**.

These two structural factors such as the extent of core space and the intramolecular repulsion between methyl chains and neighboring units have an impact on structural ordering. These results directly affect those TFT properties.

Film Morphologies. Figure 8 shows tapping mode atomic force microscopy (AFM) images of **PmT**, **PmSe**, **PTmT**, and **PTmSe** on OTS-8 modified silicon wafer substrates after annealing at 120 °C for 10 min. These AFM images of **PmSe** and **PmT** showed that they have rough granular crystalline surfaces near to amorphous. In contrast, AFM images of **PTmT** and **PTmSe** showed much larger grains than those of **PmT** and **PmSe**, consistent with a more ordered intermolecular arrangement that facilitates high carrier mobility.[36] Moreover, because of better connectivity between the neighboring domains of **PTmT** and **PTmSe**, the resulting charge carrier transports in TFT devices are expected to be very good.

TFT Properties. OTFTs based on **PmT**, **PmSe**, **PTmT**, and **PTmSe** were fabricated using solution processing. Top-contact OTFTs were fabricated on a highly n-doped silicon wafer with a 200 nm thick thermally grown SiO_2 dielectric layer. The surface of the substrate was modified with OTS-8. The semiconducting layer (thickness 40 nm) was spin-cast onto the substrate at 2500 rpm from 0.5 wt % chlorobenzene solution. Gold source and drain electrodes were deposited through a shadow mask on top of active layer. The channel length was $L = 50$ μm and the channel

(36) Lu, K.; Di, C.; Xi, H.; Liu, Y.; Yu, G.; Qiu, W.; Zhang, H.; Gao, X.; Liu, Y.; Qi, T.; Du, C.; Zhu, D. *J. Mater. Chem.* **2008**, *18*, 3426.

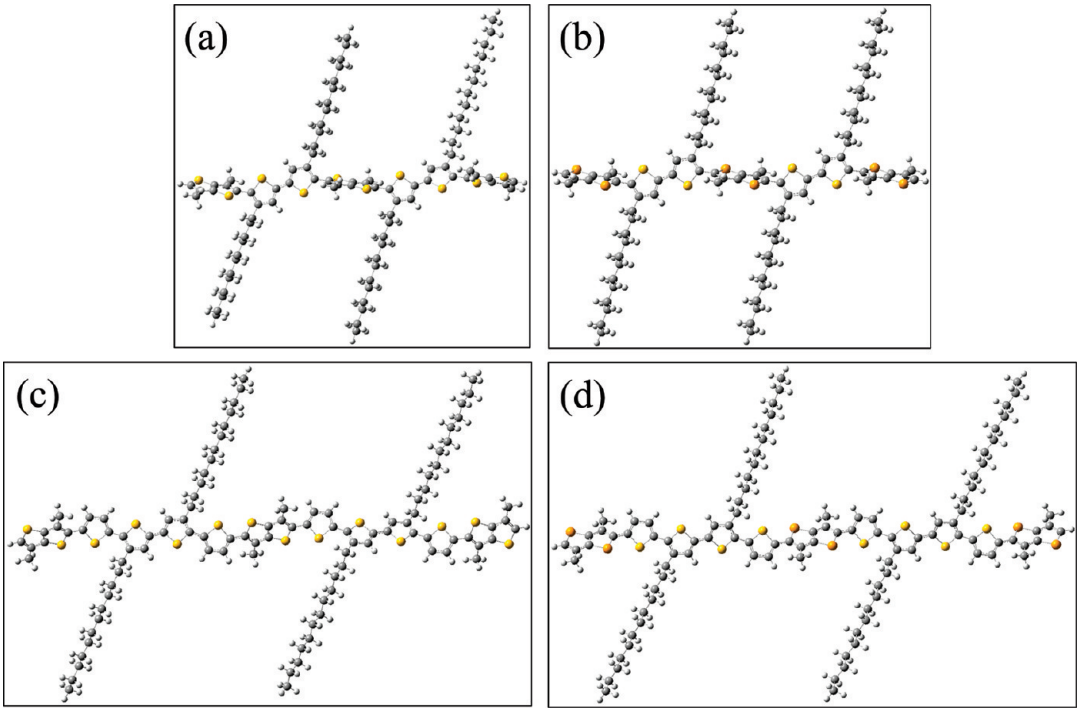

Figure 7. Geometry-optimized molecular structures obtained at the B3LYP/3-21G* calculation level: (a) **PmT**, (b) **PmSe**, (c) **PTmT**, and (d) **PTmSe.**

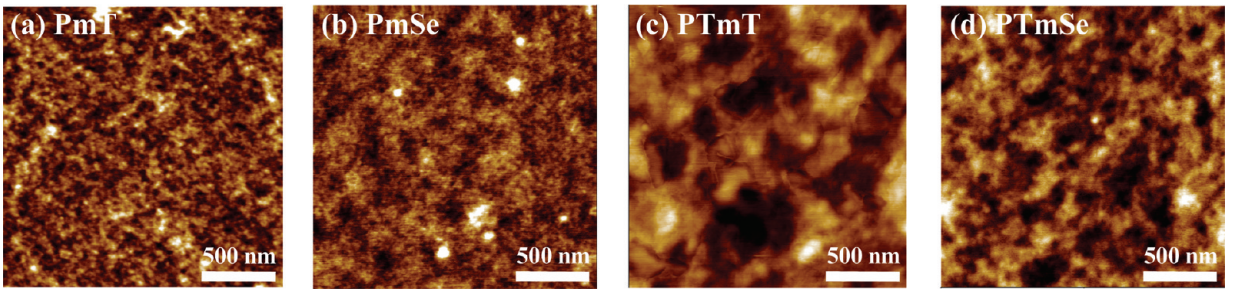

Figure 8. AFM images (2 μm × 2 μm) of (a) **PmT**, (b) **PmSe**, (c) **PTmT** and (d) **PTmSe**.

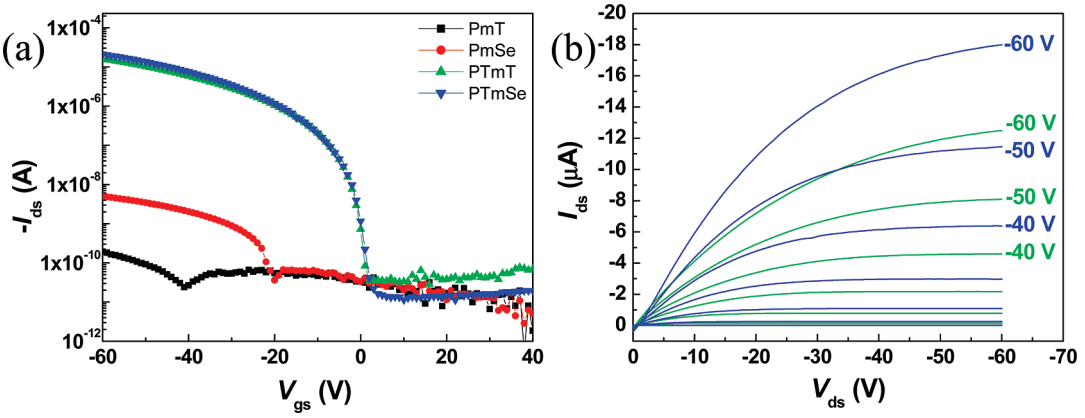

Figure 9. (a) Transfer characteristics of **PmT**, **PmSe**, **PTmT**, and **PTmSe** in the saturation regime at a constant source-drain voltage of −60 V and (b) output characteristics of **PTmT** (green line) and **PTmSe** (blue line) at various gate voltages.

width was W = 1500 μm. The OTFTs of the polymers exhibited typical p-channel FET characteristics.

Figure 9a shows the transfer characteristics of **PmT**, **PmSe**, **PTmT**, and **PTmSe**, and Figure 9b shows the output curves for **PTmT** and **PTmSe**. The mobilities, on/off ratios, and threshold voltages of the OTFTs obtained from these polymers are listed in Table 2. The TFT mobilities were calculated in the saturation regime using the following

Table 2. Performance of TFTs Based on the Polymers

polymer	mobility ($cm^2V^{-1}s^{-1}$)[a]	threshold voltage (V_{th})	on/off ratio
PmT	8.1×10^{-7}	−39	10^1
PmSe	6.4×10^{-6}	−15	10^2
PTmT	0.03	−7	10^6
PTmSe	0.04	−9	10^6

[a] Evaluated from the saturation regime at V_D = −60 V.

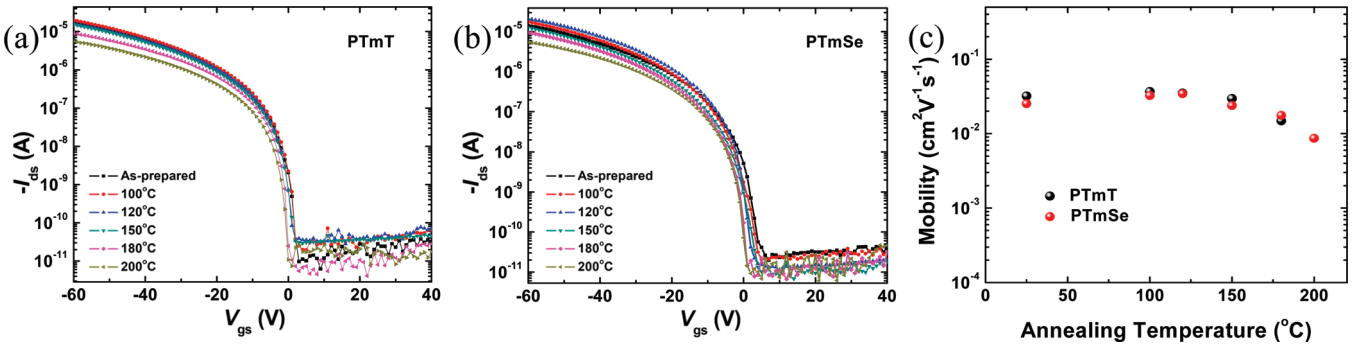

Figure 10. Transfer characteristics of (a) **PTmT** and (b) **PTmSe**, and (c) mobility plot for various annealing temperatures.

equation: $I_{ds} = (W/2L)\,\mu C_i(V_{gs} - V_{th})^2$, where I_{ds} is the drain-source current in the saturated region, W and L are the channel width and length, respectively, μ is the field-effect mobility, C_i is the capacitance per unit area of the insulation layer, and V_{gs} and V_{th} are the gate and threshold voltages, respectively.[2] Although the mobility of **PmSe** (6.4×10^{-6} cm^2 V^{-1} s^{-1}) was very slightly higher than that of **PmT** (8.1×10^{-7} cm^2 V^{-1} s^{-1}), the TFT performances of these two polymers were very poor. Moreover, the threshold voltages (V_{th}) obtained from the transfer curves for **PmT** and **PmSe** were −39 and −15 V, respectively, indicating a relatively high density of charge carrier traps. As discussed in the previous section, the inter- and intramolecular repulsion of the polymers result in rotational distortion of the fused aromatic core units, causing degradation of the intermolecular ordering. In contrast, the **PTmT** and **PTmSe** devices exhibited much superior mobilities, $\mu = 0.03$−0.04 cm^2 V^{-1} s^{-1}, with a high on/off ratio of 10^6. In addition, the transfer curves of these polymers exhibited small threshold voltages of −7 to −9 and a near zero turn-on voltage. The output curves of **PTmT** and **PTmSe** FETs showed very good saturation behavior and no contact resistance. However, similarly to the relationship between **PmT** and **PmSe**, although **PTmSe** showed slightly improved TFT mobility and drain current in output curves compared to **PTmT**, there was no big difference by the sulfur or selenium atom. TFT results rather were significantly dependent on the structural ordering. Although the only difference between **PTmSe** (or **PTmT**) and **PmSe** (or **PmT**) is the presence of additional thiophene rings in the polymer main backbone of the former, these additional thiophene rings play an important role in structural ordering. This result is consistent with those of the UV, CV, AFM, and XRD measurements. The improved intermolecular ordering increases the effective conjugation length of **PTmSe**, which directly affects its performance in TFTs.

We also investigated the effects annealing on the TFT characteristics of **PTmT** and **PTmSe**. The **PTmT** and **PTmSe** TFT devices were basically annealed at 120 °C and additionally annealed at other temperatures. Figure 10 shows the TFT results for the as-cast and for devices annealed at various temperatures. The mobilities of the spin-coated films for these polymers at room temperature were about 0.03 cm^2 V^{-1} s^{-1} with an on/off ratio of the order of 10^6. After annealing at 100 and 120 °C, the mobility of **PTmSe** was very slightly improved to values as high as 0.04 cm^2 V^{-1} s^{-1}. When both devices for **PTmT** and **PTmSe** were annealed at 200 °C, the mobilities slightly decreased to 0.01 cm^2 V^{-1} s^{-1}. In addition, the transfer curves of **PTmT** and **PTmSe** devices annealed at various temperatures indicated good thermal stability, with little variation in the on/off current and threshold voltage with annealing temperature.

Conclusion

A series of new semiconducting polymers containing fused aromatic rings were successfully synthesized via $FeCl_3$-mediated oxidative coupling polymerization. Although the polymer structures of **PmT** and **PmSe** are similar to that of PBTTT, their TFT performances are poor because of the distortion of the core units caused by inter- and intramolecular repulsion between long dodecyl side chains and methyl chains attached to the core units. In contrast, **PTmT** and **PTmSe** containing the additional unsubstituted thiophene rings next to the fused aromatic core units exhibited well ordered intermolecular structures. These additional thiophene rings retain planarity of the polymer main backbone by diminishing the distortion of the rigid core units, enable intermolecular interdigitation of the dodecyl side chains, and increase the conjugation length. As a result, **PTmT** and **PTmSe** exhibited very interesting optical and electrical properties and significantly improved TFT performance with a charge carrier mobility of 0.03−0.04 cm^2 V^{-1} s^{-1} (on/off ratio = 10^6), compared to **PmT** and **PmSe**. Post-deposition annealing of **PTmT** and **PTmSe** devices resulted in little change in the TFT performance, indicating good thermal stability. Thus both polymers, **PTmT** and **PTmSe**, can be considered for use as a semiconductor to realize high-performance and stable OTFTs that can be fabricated at low temperature using solution processing.

Acknowledgment. This work was supported by a grant (F0004011-2008-31) from the Information Display R&D Center, one of the 21st Century Frontier R&D Programs funded by the Ministry of Commerce, Industry, and Energy of the Korean Government. Work at UCSB was supported by the Heeger Center for Advanced Materials at the Gwangju Institute of Science and Technology and by the GRL Program of the Korean Government (M60605000005-06A0500-00510). We thank Professor Alan J. Heeger for discussions and for advice on the manuscript.